Performance of recent and high-performance approximate density functionals for time-dependent density functional theory calculations of valence and Rydberg electronic transition energies

Miho Isegawa, Roberto Peverati, and Donald G. Truhlar

Re-register for Table of Content Alerts

Create a profile. Sign up today!

Performance of recent and high-performance approximate density functionals for time-dependent density functional theory calculations of valence and Rydberg electronic transition energies

Miho Isegawa, Roberto Peverati, and Donald G. Truhlar
Department of Chemistry and Supercomputing Institute, University of Minnesota, Minneapolis, Minnesota 55455-0431, USA

We report a test of 30 density functionals, including several recent ones, for their predictions of 69 singlet-to-singlet excitation energies of 11 molecules. The reference values are experimental results collected by Caricato *et al.* for 30 valence excitations and 39 Rydberg excitations. All calculations employ time-dependent density functional theory in the adiabatic, linear-response approximation. As far as reasonable, all of the assignments are performed by essentially the same protocol as used by Caricato *et al.*, and this allows us to merge our mean unsigned errors (MUEs) with the ones they calculated for both density functional and wave function methods. We find 21 of the 30 density functionals calculated here have smaller MUEs for the 30 valence states than what they obtained (0.47 eV) for the state-of-the-art EOM-CCSD wave function. In contrast, for all of density functionals the MUE for 39 Rydberg states is larger than that (0.11 eV) of EOM-CCSD. Merging the 30 density functionals calculated here with the 26 calculated by Caricato *et al.* makes a set of 56 density functionals. Averaging the unsigned errors over both the valence excitations and the Rydberg excitations, none of the 56 density functionals shows a lower mean unsigned error than that (0.27 eV) of EOM-CCSD. Nevertheless, two functionals are successful in having an overall mean unsigned error of 0.30 eV, and another nine are moderately successful in having overall mean unsigned errors in the range 0.32–0.36 eV. Successful or moderately successful density functionals include seven hybrid density functionals with 41% to 54% Hartree–Fock exchange, and four range-separated hybrid density functionals in which the percentage of Hartree–Fock exchange increases from 0% to 19% at small interelectronic separation to 65%–100% at long range. © *2012 American Institute of Physics.*
[http://dx.doi.org/10.1063/1.4769078]

I. INTRODUCTION

As quantum chemistry is applied to increasingly complex problems involving solar energy, synthetic, mechanistic, and environmental photochemistry, photocatalysis, photoelectrochemistry, laser control, photophysics, vision and photosynthesis, luminescence, and photoabsorption and emission in various media, the large size, and complexity of many of the molecules involved make time-dependent density functional theory[1–4] (TDDFT) the method of choice for calculating electronic excitation energies and the potential surfaces of excited electronic states. This drives a demand for validation studies of TDDFT for all kinds of excitations, and these studies need to be updated as improved approximate density functionals are developed.

Each validation study is based on a set of benchmark electronic excitation energies for diverse kinds of molecules and excitations, including valence, Rydberg, and charge transfer excitations, as well as excitations with two or more of these prototype characteristics. While much has been learned from the many papers considering individual systems or a few related systems, more general conclusions can be drawn from studies involving a large set of data, here called a database. One particularly complete study[5] included 29 density functionals applied to 103 gas-phase excitations of 28 molecules

(based on theoretical reference data of Thiel and co-workers[6]) and 614 liquid-phase excitations of 483 molecules (based on experimental data, including many dyes and large chromogens). The comparisons in the liquid phase suffer from the difficulty of accurately estimating the contributions of the various solvents, and in fact more accurate methods for solvatochromic shifts were developed subsequently.[7] The excitations in the 103-state and 614-state sets were mainly valence states, but the database was later extended to include Rydberg and charge transfer excitations;[8,9] and reference data on cyanine dyes were improved, leading to improved conclusions about the accuracy of TDDFT.[10] The extended database has also been applied to some new functionals, first[8] to M06-L,[11] M06-HF,[12] M06,[13] and M06-2X[14] (published in 2006–2008) then[9] to M08-HX[14] and M08-SO[14] (published in 2008), and then[15] to M11[9] and M11-L[16] (published in 2011–2012), and finally to N12,[17] MN12-L,[18] N12-SX,[19] and MN12-SX,[19] and to the older HSE functional[20] (published in 2003).

Caricato *et al.* published a second large database, this one based on experimental gas-phase data and including 30 valence states and 39 Rydberg states of 11 molecules.[21] and they used it to test 26 approximate density functionals published from 1951 to early 2006. Whereas the previously discussed data sets were dominated by valence excitations, this database has about half Rydberg excitations.

Since this database provides coverage complementary to the data described in the previous paragraph, it provides a useful independent test, and in the present work we use it to examine the performance of 30 recent approximate density functionals.

A couple of additional large validation studies may also be mentioned[22, 23] but will not be considered in the present work. Most of the applications and validation studies of TDDFT have employed adiabatic, linear-response TDDFT based on perturbing the ground-state Kohn–Sham determinant by a time-dependent electric field and have examined only the performance for vertical singlet-to-singlet excitations, and we shall limit ourselves in that way here as well; we refer the reader elsewhere for discussions of more advanced versions of TDDFT[24–28] or more general initial states.[29–32] We also note that TDDFT is not the only way to apply density functional theory (DFT) to excited states. For example, there are also methods involving self-consistent field calculations on excited-states;[29, 33, 34] these methods are very promising but are beyond the present scope to discuss.

II. COMPUTATIONAL DETAILS

Geometries were optimized for the ground state of each molecule by MP2/6-311+G**. All TDDFT calculations were carried out with a 6-311(2+,2+)G** basis as proposed by Wiberg *et al.*[35] (the angular momentum quantum numbers and exponential parameters of the additional four diffuse subshells are s(H), 0.00108434; sp(C), 0.0131928; sp(O), 0.025451869; sp(N), 0.0192470). Extensive calculations were also performed with both more and less diffuse functions; although the results show a small dependence on basis set, it was decided that 6-311(2+,2+)G** is adequate with the exception of one state discussed in Sec. II A, and we report results with only this one basis set. All the calculations were performed with a locally modified[36] version of the GAUSSIAN 09 program.[37]

We chose the functionals to include in this work in order to complement the results obtained by Caricato *et al.*[21] and therefore we first considered the ten Minnesota meta functionals mentioned above (M06-L, M06, M06-2X, M06-HF, M08-HX, M08-SO, M11-L, M11, MN12-L,[18] and MN12-SX[19]), the recent SOGGA11,[38] SOGGA11-X,[39] N12,[17] and N12-SX[19] gradient approximation functionals, and the ωB97 family of functionals of Chai and Head-Gordon (ωB97,[40] ωB97X,[40] and ωB97X-D[41]). Since Caricato *et al.*[21] found that functionals with a high percentage of HF exchange are the most successful functionals for this database, we also included four older functionals with high percentages of Hartree–Fock (HF) exchange, namely, MPW1K,[42] MPWB1K,[43] MPWKCIS1K,[44] and PWB6K.[45]

We also considered two HCTH-type family of GGAs: HCTH/93[46] and HCTH/147[46] and the dispersion-corrected B97-D GGA.[47]

For B97-D, M06-L, HCTH/93, HCTH/147, HCTH/407,[48] and τ-HCTH[49] we also considered applying Hirao's long-range correction[50] in which the two-electron

repulsion operator is given by

$$\frac{1}{r_{12}} = \frac{1 - \mathrm{erf}(\mu r_{12})}{r_{12}} + \frac{\mathrm{erf}(\mu r_{12})}{r_{12}}, \qquad (1)$$

where the short-range part is treated by a local exchange functional, and the long-range part is treated by the Hartree–Fock exchange equations with Kohn–Sham orbitals; μ is parameter that ideally should be optimized for each GGA. However, in the present study, we used the value, 0.47 a_0^{-1}, which was optimized by Song *et al.* (they optimized it for atomization energies).[51]

Some of the other functionals considered here are also range separated; thus ωB97 and ωB97X are range-separated-hybrid GGAs, while ωB97X-D is a range-separated-hybrid GGA augmented with a damped dispersion molecular mechanics term; in these functionals the percentage of Hartree–Fock exchange increases from respectively 0 (ωB97), 15.7706 (ωB97X), and 22.2036 (ωB97X-D) at small interelectronic separation to 100 at large interelectronic separations. In the ωB97X-D functional, the damped dispersion term has no direct effect on the excitation energies because the parameters are assumed to be independent of state, but the results are still different from ωB97X because the other parameters were optimized[41] in the presence of damped dispersion. M11 is also range separated with the percentage of Hartree–Fock exchange increasing from 42.8 at small interelectronic separation to 100 at large interelectronic separation. M11-L is range-separated but with local (but different) exchange approximations at small and large interelectronic separations. N12-SX and MN12-SX are, respectively, a range-separated nonseparable gradient approximation (NGA) and a range-separated meta NGA, where, as in the HSE functional, the percentage of Hartree–Fock exchange decreases from 25 at small interelectronic separation to 0 at large interelectronic separation; functionals with Hartree–Fock exchange increasing to 100% at large interelectronic distance are called long-range corrected (LC), whereas those with Hartree–Fock exchange decreasing to zero are called screened exchange (SX) functionals.

In most molecules, the majority of low-lying states are Rydberg states or Rydberg-like states. In many cases the assignment of the calculated TDDFT transitions is not unambiguous because some high-energy states are over-stabilized by the incorrect asymptotic behavior of the exchange-correlation potential, and they incorrectly appear at energies comparable to those of the low-energy transitions of interest. This is a general problem with TDDFT when one considers a range of excitation energies for a given molecule rather than just the lowest one or two states, and the problem is especially serious for local functionals and for functionals with a small percentage of HF exchange (less than about 30%–35%). Moreover, the problem is exacerbated when large and diffuse basis sets are used, but one needs to use such well-augmented basis sets in order to treat the Rydberg states correctly. Using a less diffuse basis set usually reduces the number of available high-energy states and therefore reduces the contamination and improves the SCF convergence; for

this reason, a calculation with a smaller basis set might help with the assignments (and one can possibly even obtain more accurate results for the pure valence states), but it can deteriorate the quality of the results for the entire spectrum including the Rydberg states. The basis set we selected (specified above) is a compromise in the light of these conflicting demands.

The problem of the contamination of the low-energy spectrum by the spuriously lowered high-energy spectrum is well known in TDDFT and is understood at the theoretical level.[52–56] The spuriously lowered states are usually charge transfer states.[57–59] The use of a moderate or high percentage of HF exchange (by means of using a global hybrid functional or range-separated hybrid functional) ameliorates the problem; however, it remains troublesome in practical work, and if the percentage of Hartree–Fock exchange is too high, the calculations may suffer from unacceptably large static correlation error. The charge transfer states that we call spurious may actually be real charge transfer states, but their energy is predicted to be much too low by methods with zero X or low X, and they are spurious in the sense that they do not belong in the low-energy spectrum.

Sometimes one can distinguish the valence states from the spuriously lowered TDDFT states because the valence states have non-negligible oscillator strengths, whereas the spuriously lowered TDDFT states usually have negligible oscillator strengths, but this is not a general procedure because some molecules, e.g., s-tetrazine, have valence states with small or zero oscillator strength; furthermore, the real Rydberg states and some charge transfer states also have small or negligible oscillator strengths, and they can be harder to distinguish visually from the spuriously lowered states. It turns out that 9 of the 11 molecules in the present database have valence states with zero oscillator strength for at least one irreducible representation (irrep). Herbert has pointed out,[57] "Thus the real dark states cannot be identified simply from a list of excitation energies and oscillator strengths, but only by careful analysis of the MOs or (better yet) attachment/detachment densities. In larger clusters, however, CT states can undergo a type of ersatz intensity borrowing that greatly complicates interpretation of the vertical excitation spectrum." We agree; therefore, we did not use oscillator strengths in making the assignments.

One technique we used to distinguish spurious from real calculated states in recent past work[15] was to look at the coefficients of the single excitations in a given transition and compare them to those of a calculation with less or no spurious states, e.g., a calculation with the M06-HF functional. However, as we tried to apply this method in the present work, where there are more Rydberg states and more troublesome functionals (especially, SOGGA11, M06-L, M11-L, N12, MN12-L, M06, and MN12-SX) than in the previous study, that we decided to switch to the scheme used by Caricato *et al.* They explained this procedure as follows:[21] "The assignment of the valence states . . . was checked by looking at the orbitals mainly involved in the transition (for low lying states, only few orbitals are involved . . .). The Rydberg states are more difficult to assign. We put those states in energy order within each irreducible representation for each method

and each molecule, and matched them against the experimental data, sorted in the same manner." This method is directly relevant to the common situation in real applications to complex systems where one has no advance knowledge of what states to look for in the TDDFT spectrum, and one has to consider each predicted state as a potentially real one. Two other advantages of following their procedure are that it is less ambiguous than other procedures we attempted, and it allows us to merge our tables of mean unassigned errors with their tables and thereby obtain a more comprehensive view in which a greater number of functionals are compare for the same set of data.

An additional consideration in making the assignments is that real valence states are often mixed to a greater or lesser extent with Rydberg states,[60] so one must accept such mixed states as potential candidates for the nominal valence states when interpreting the results of TDDFT calculations. Another complication in the artificial division of a spectrum into valence states, Rydberg states, and charge transfer states is the presence in spectra of σ^* antibonding states, which are non-π^* valence states that often correlate with Rydberg states of the united atoms formed by coalescing hydrogen atoms into their bonding partners. The non-π^* states in the low-energy spectra considered here are mainly Rydberg nonbonding states, and we will simply call them Rydberg states without attempting to specifically distinguish any participation of antibonding character. Because the assignments are a key issue in a study like this, we here summarize the procedure we used in more detail; the procedure has two steps. In the first step, we visualize the orbitals of the states that are candidates for classification as valence states, and we classify each relevant unoccupied orbital as either a π^* orbital or a nonvalence orbital (where the latter includes mainly Rydberg orbitals); this is straightforward because in the present database almost all the valence unoccupied orbitals are relatively easily distinguished from nonvalence orbitals. Then we classify the states into two groups. If a calculated state includes significant (even if small) amplitude corresponding to an excitation to π^* valence orbital, the state is classified as a valence state; if the final state orbitals of all significantly contributing single-excitation transition amplitudes are Rydberg orbitals, the state is classified as a nonvalence state (which is a Rydberg state, a charge transfer state, or an excitation to a σ^* orbital). In the next step, the states in each group are ordered according to their calculated energy within each irrep and directly compared in the calculated order to the experimental data for that group and that irrep in order of increasing energy, irrespective of the character of each state (except for irrep and except for the group to which it is assigned) and without excluding any state.

An advantage of the method we use for assignments that it gives a useful evaluation of the performance in predicting the whole low-energy spectrum. Notice that the results obtained by this method sometimes have a special dependence on the basis set because a calculation with a more diffuse basis set can over-stabilize more high-energy states and therefore present a denser low-energy spectrum, with a consequently different performance. We used a different basis set than Caricato *et al.*, but we made extensive basis set tests, and we do

not believe that any of our conclusions are sensitive to this difference, especially since the basis-set dependence is greatest for functionals that would not be recommended for spectra containing both valence and Rydberg states based on any reasonable way of measuring their performance.

III. RESULTS AND DISCUSSION

In this section, we present the results of our calculations and a discussion of the reliability of the considered functionals. In all cases, we used the same experimental data and assignments of experimental lines as presented by Caricato *et al.*[21] The reader should be cautioned that statistical analyses of the type below are not a perfect method of assessment because, for example, they do not take account of the error bars in extracting excitation energies from experiment (these error bars are hard to assess, but they are larger in the heterocycles because there is a strong vibronic contribution). We nevertheless lean heavily on statistical analysis because with so many molecules and so many density functionals some statistics are required to grasp the main trends. The discussion of individual molecules is important as well, and a balanced assessment involves both discussions and statistics, as provided below. Once one decides to use statistics, the question comes up of whether to use maximum error (MaxE) or root mean squared error, both of which have their place. We chose mean unsigned error (MUE) for the discussion because of its robustness for non-normally distributed errors, but we provide MaxE values in the supplementary material.[61]

As a rough guide, we consider functionals with MUEs of 0.30 eV or less as successful, those with MUEs up to 20% larger (0.31–0.36 eV) as moderately successful, and those with a MUE > 0.36 eV as unsuccessful. Of course one would like to do even better, but Caricato *et al.* found that even the EOM-CCSD method,[62] which is much more expensive than density functional theory and is usually considered a method of choice among practical wave function methods for small and medium-sized molecules (unlike TDDFT, it is usually unaffordable for large molecules), has a MUE of 0.27 eV for the 69 excitation energies in the database under consideration here, so accuracies in that ballpark must be considered as competitively useful for applications to large and complex systems; and we placed the outfield wall of the ballpark at 0.36 eV (such a choice is necessarily somewhat arbitrary, but defining a criterion of success provides needed structure to the discussion).

In Tables I–XI, the density functionals are ordered according to their percentage of HF exchange. Although we tested 30 new functionals in the present paper, Tables I–XI include only 22 of them, in order to keep the tables to a manageable size. Versions of Tables I–XI containing all 30 newly tested functionals are given in the supplementary material.[61] The eight functionals included in supplementary material that are not included in Tables I–XI of the paper are: B97–D, HCTH/147, LC-B97-D, LC-HCTH/147, LC-HCTH/407, LC-τ-HCTH, N12, and MN12-L; these functionals are, however, included in Table XII.

A. Alkenes and butadiene

1. Ethylene

Table I shows signed deviations of the calculated excitation energies from the experimental values for the ethylene molecule (point group D_{2h}). For this molecule, one valence transition and ten Rydberg transitions are assigned. For all of the density functionals, the lowest calculated transition energy of the B_{1u} irrep is assigned to the B_{1u} $\pi \rightarrow \pi^*$ valence transition; for most density functionals this corresponds to excitation from the highest occupied molecular orbital (HOMO) to higher virtual orbitals than the lowest unoccupied molecular orbital (LUMO); only the calculation by M06-L includes a significant contribution of HOMO–LUMO excitation. An oscillator strength greater than 0.1 is obtained for all examined density functionals except SOGGA11. The ten Rydberg states are assigned in order of increasing energy for each considered symmetry starting from the lowest transition energy. Since the lowest transition energy $1B_{1u}$ is assigned as a valence transition $\pi \rightarrow \pi^*$, the second lowest energy is assigned as the B_{1u} Rydberg state.

The best performance for ethylene is provided by ωB97X for which the error of the one valence state is 0.04 eV, and the MUE of ten Rydberg states is 0.24 eV, and—using the 0.30 eV criterion defined above—only this functional is successful for Rydberg states, although M06-HF, MPWB1K, and PWB6K have MUEs of 0.34, 0.38, and 0.39 eV, respectively, for the Rydberg states so they are almost good enough to be called successful. Large errors are observed for local density functionals (HCTH/93, SOGGA11, M06-L, and M11-L) and for M06, which has only 27% Hartree–Fock exchange.

Most of the density functionals underestimate the transition energy for both valence and Rydberg states, i.e., most of the errors in Table I are negative. However the error for the $5B_{3u}$ state, which is a high-principal-quantum-number Rydberg state, is large and positive for several of the better performing density functionals. This is the state (of all the states considered in this paper, including those for other molecules discussed below) that is most sensitive to increasing the basis set from 6-311(2+,2+)G** to 6-311(3+,3+)G**, and using the latter basis set does lower the energy of the $5B_{3u}$ state; however, this triply augmented basis set makes some of the lower-energy states less accurate, so we decided to use the 6-311(2+,2+)G** basis set consistently for all of our analysis, even though it may be insufficient for this one high-principal-quantum-number Rydberg state. For other molecules considered below, the two basis sets typically agree within at most a few hundredths of an eV and often agree to better than 0.01 eV.

2. Isobutene

Table II gives the signed errors of the vertical transition energies for isobutene (point group C_{2v}). Two Rydberg states (B_1 and A_1) are considered for this molecule, and they are each assigned as the lowest energy state in their irrep. The Rydberg states for this molecule are well predicted by many of the density functionals; the mean unsigned error is below 0.3 eV for eight of 17 density functionals. The lowest error

TABLE I. Signed errors of vertical electronic excitation energies (eV) for the calculated states of ethylene, and mean unsigned errors (MUEs) for the ten Rydberg states.

	X^a	$1B_{3u}$ Ryd	$1B_{1u}$ Val (π-π^*)	$1B_{1g}$ Ryd	$1B_{2g}$ Ryd	$2A_g$ Ryd	$2B_{3u}$ Ryd	$3B_{3u}$ Ryd	$4B_{3u}$ Ryd	$3B_{1g}$ Ryd	$2B_{1u}$ Ryd	$5B_{3u}$ Ryd	MUE(10) Ryd
HCTH/93	0	−0.93	−0.51	−1.17	−1.32	−1.35	−1.35	−1.53	−1.04	−1.35	−1.46	−0.07	1.16
M06-L	0	−0.44	−0.21	−0.84	−0.97	−0.36	−0.92	−1.08	0.04	−1.09	−1.27	0.56	0.76
SOGGA11	0	−1.62	−1.74	−2.22	−2.32	−2.25	−2.49	−1.66	−0.77	−1.42	−1.82	−0.20	1.68
M11-L	0	−1.78	−1.04	−2.07	−2.27	−1.75	−1.92	−1.41	−1.47	−1.51	−1.71	−0.52	1.64
N12-SX	25–0	−0.63	−0.34	−0.86	−0.97	−0.98	−0.90	−1.12	−0.70	−1.12	−1.22	0.26	0.87
MN12-SX	25–0	−1.96	−1.07	−2.28	−2.43	−1.87	−2.09	−1.50	−1.50	−1.34	−1.57	−0.59	1.71
M06	27	−1.19	−0.70	−1.48	−1.58	−1.37	−1.43	−1.26	−1.20	−1.42	−1.49	−0.27	1.27
SOGGA11-X	40.15	−0.35	−0.20	−0.49	−0.57	−0.66	−0.49	−0.59	−0.38	−0.75	−0.81	0.58	0.57
MPWKCIS1K	41	−0.26	−0.17	−0.39	−0.46	−0.50	−0.39	−0.53	−0.30	−0.75	−0.70	0.57	0.49
MPW1K	42.8	−0.12	−0.11	−0.24	−0.31	−0.38	−0.27	−0.38	−0.17	−0.61	−0.60	0.71	0.38
MPWB1K	44	−0.23	−0.14	−0.36	−0.42	−0.49	−0.37	−0.50	−0.28	−0.72	−0.68	0.61	0.47
PWB6K	46	−0.18	−0.14	−0.27	−0.32	−0.42	−0.28	−0.39	−0.21	−0.63	−0.59	0.63	0.39
M08-HX	52.23	−0.73	−0.33	−0.85	−0.90	−0.79	−0.66	−0.39	−0.42	−0.40	−0.57	0.42	0.61
M06-2X	54	−0.28	−0.14	−0.46	−0.49	−0.47	−0.42	−0.38	−0.33	−0.54	−0.64	0.57	0.46
M08-SO	56.79	−0.76	−0.42	−0.95	−0.98	−0.72	−0.78	−0.38	−0.46	−0.44	−0.68	0.34	0.65
LC-HCTH/93	0–100	0.38	−0.07	0.40	0.49	0.38	0.58	0.67	0.52	0.48	0.38	1.36	0.57
LC-M06-L	0–100	1.20	0.26	0.51	1.48	1.35	1.21	1.42	1.39	0.90	1.08	2.29	1.28
ωB97	0–100	0.41	−0.01	0.35	0.38	0.23	0.35	0.34	0.39	0.20	0.03	1.32	0.4
ωB97X	15.77–100	0.22	−0.04	0.18	0.20	0.03	0.17	0.13	0.20	−0.03	−0.13	1.12	0.24
ωB97X-D	22.2–100	−0.17	−0.14	−0.29	−0.32	−0.49	−0.33	−0.42	−0.24	−0.53	−0.68	0.74	0.42
M11	42.8–100	−0.62	−0.27	−0.87	−0.88	−0.63	−0.69	−0.26	−0.17	−0.14	−0.63	0.60	0.55
M06-HF	100	−0.43	−0.23	−0.58	−0.48	−0.38	−0.34	−0.09	0.10	0.13	−0.18	0.73	0.34
Expt.		7.11	7.65	7.80	7.90	8.28	8.62	8.90	9.08	9.20	9.33	9.51	

[a] In all tables, X is the percentage of Hartree–Fock exchange. When a range of X is indicated, the first value corresponds to small interelectronic separations, and the second to large interelectronic separations.

TABLE II. Signed errors of vertical electronic excitation energies (eV) for the calculated states of isobutene, and mean unsigned errors (MUEs) for the two Rydberg states.

	X	B_1 Ryd	A_1 Ryd	MUE(2) Ryd
HCTH/93	0	−0.98	−0.95	0.96
M06-L	0	−0.54	−0.64	0.59
SOGGA11	0	−1.77	−1.88	1.82
M11-L	0	−1.89	−1.72	1.80
N12-SX	25–0	−0.59	−0.57	0.58
MN12-SX	25–0	−2.00	−1.90	1.95
M06	27	−1.12	−1.08	1.10
SOGGA11-X	40.15	−0.19	−0.23	0.21
MPWKCIS1K	41	−0.15	−0.16	0.15
MPW1K	42.8	0.04	−0.03	0.03
MPWB1K	44	−0.06	−0.10	0.08
PWB6K	46	−0.04	−0.06	0.05
M08-HX	52.23	−0.60	−0.52	0.56
M06-2X	54	−0.13	−0.15	0.14
M08-SO	56.79	−0.60	−0.53	0.57
LC-HCTH/93	0–100	0.62	0.33	0.47
LC-M06-L	0–100	1.24	0.69	0.97
ωB97	0–100	0.64	0.34	0.49
ωB97X	15.77–100	0.43	0.23	0.33
ωB97X-D	22.2–100	0.04	−0.06	0.05
M11	42.8–100	−0.40	−0.40	0.40
M06-HF	100	−0.08	−0.09	0.08
Expt.		6.17	6.70	

is seen in MPW1K with the MUE being only 0.03 eV, and PWB6K, ωB97X-D, MPWB1K, and M06-HF also show MUEs below 0.1 eV.

3. Trans-1,3-butadiene

Table III gives the signed errors of vertical transition energies for trans-1,3-butadiene (point group C_{2h}). For this molecule, we consider one valence state, which is a B_u $\pi \to \pi^*$ state, and it is assigned to the lowest calculated B_u transition energy for all density functionals.

All of the density functionals have an error below 0.30 eV for the valence state except for four local density functionals (HCTH/93, SOGGA11, M06-L, and M11-L) and the nonlocal density functional that contains small percentage Hartree–Fock exchange (N12-SX (25% for short range), MN12-SX (25% for short range), and M06 (27%)). The minimum MUE for Rydberg states is 0.20 eV, achieved by ωB97X-D. MPW1K, MPWB1K, and PWB6K also perform very well for Rydberg states. M06-L shows the best performance among the three local density functionals for both valence and Rydberg states, but the performance is not good enough to be useful.

B. Carbonyls

The results for four valence excitations and 21 Rydberg states of three carbonyl compounds are reported in Tables IV–VI.

TABLE III. Signed errors of vertical electronic excitation energies (eV) for the calculated states of trans-1,3-butadiene, and mean unsigned errors (MUEs) for the six Rydberg states.

	X	$1B_u$ Val (π-π^*)	$1B_g$ Ryd	$2A_u$ Ryd	$2B_u$ Ryd	$2B_g$ Ryd	$3A_g$ Ryd	$3B_u$ Ryd	MUE(6) Ryd
HCTH/93	0	−0.53	−0.96	−1.14	−0.96	−1.30	−1.22	−1.11	1.11
M06-L	0	−0.26	−0.58	−0.81	−0.73	−1.07	−0.97	−0.90	0.84
SOGGA11	0	−0.54	−1.59	−1.84	−1.44	−2.26	−1.76	−1.76	1.78
M11-L	0	−0.83	−1.86	−2.05	−1.42	−2.14	−1.67	−1.39	1.75
N12-SX	25–0	−0.35	−0.72	−0.86	−0.75	−1.00	−0.95	−0.83	0.85
MN12-SX	25–0	−0.96	−2.14	−2.28	−1.36	−2.42	−1.93	−1.61	1.96
M06	27	−0.58	−1.28	−1.38	−1.22	−1.53	−1.32	−1.17	1.32
SOGGA11-X	40.15	−0.19	−0.46	−0.53	−0.59	−0.78	−0.62	−0.50	0.58
MPWKCIS1K	41	−0.17	−0.32	−0.38	−0.32	−0.46	−0.41	−0.25	0.36
MPW1K	42.8	−0.12	−0.18	−0.24	−0.22	−0.33	−0.31	−0.15	0.24
MPWB1K	44	−0.13	−0.27	−0.30	0.17	−0.40	0.28	0.02	0.24
PWB6K	46	−0.13	−0.23	−0.28	0.20	−0.52	−0.20	−0.05	0.24
M08-HX	52.23	−0.26	−0.83	−0.82	−0.58	−0.81	−0.63	−0.24	0.65
M06-2X	54	−0.12	−0.34	−0.38	−0.35	−0.48	−0.41	−0.22	0.36
M08-SO	56.79	−0.29	−0.84	−0.85	−0.62	−0.90	−0.62	−0.30	0.69
LC-HCTH/93	0–100	0.06	0.40	0.51	0.49	0.54	0.60	0.83	0.56
LC-M06-L	0–100	0.25	1.28	1.23	1.57	1.27	1.00	1.55	1.32
ωB97	0–100	0.07	0.43	0.47	0.35	0.36	0.36	0.52	0.41
ωB97X	15.77–100	−0.01	0.25	0.30	0.21	0.21	0.21	0.38	0.26
ωB97X-D	22.2–100	−0.14	−0.14	−0.13	−0.25	−0.26	−0.30	−0.12	0.20
M11	42.8–100	−0.12	−0.68	−0.67	−0.56	−0.79	−0.51	−0.20	0.57
M06-HF	100	−0.03	−0.47	−0.40	−0.28	−0.45	−0.22	0.13	0.33
Expt.		5.91	6.22	6.66	7.07	7.36	7.62	8.00	

TABLE IV. Signed errors of vertical electronic excitation energies (eV) for the calculated states of formaldehyde, and mean unsigned errors (MUEs) for the two valence states and the nine Rydberg states.

	X	$1A_2$ Val (n-π^*)	$1B_2$ Ryd	$2B_2$ Ryd	$2A_1$ Ryd	$2A_2$ Ryd	$3B_2$ Ryd	$1B_1$[a] Val (π-π^*)	$3A_2$ Ryd	$4B_2$ Ryd	$4A_1$ Ryd	$5B_2$ Ryd	MUE(2) Val	MUE(9) Ryd
HCTH/93	0	−0.09	−1.41	−1.53	−1.83	−1.80	−2.09	−0.07	−1.33	−1.57	−1.79	−1.81	0.08	1.68
M06-L	0	0.27	−0.92	−1.13	−1.49	−1.45	−1.74	0.25	−0.95	−1.08	−1.32	−1.40	0.26	1.28
SOGGA11	0	−0.28	−2.43	−2.99	−3.04	−3.28	−2.81	−0.32	−2.80	−3.06	−2.26	−2.81	0.30	2.83
M11-L	0	0.32	−2.01	−2.15	−2.27	−2.31	−1.86	0.12	−1.80	−1.95	−1.88	−2.17	0.22	2.04
N12-SX	25–0	−0.10	−0.65	−0.73	−0.99	−0.96	−1.05	−0.17	−0.54	−0.71	−1.00	−1.05	0.14	0.85
MN12-SX	25–0	0.12	−1.81	−1.97	−2.11	−2.19	−1.68	0.13	−1.66	−1.73	−1.61	−1.88	0.12	1.85
M06	27	−0.14	−1.17	−1.34	−1.50	−1.60	−1.19	−0.25	−1.15	−1.38	−1.40	−1.54	0.19	1.36
SOGGA11-X	40.15	0.06	−0.03	−0.22	−0.32	−0.33	−0.17	0.23	0.04	−0.09	−0.33	−0.43	0.15	0.22
MPWKCIS1K	41	−0.07	0.01	−0.11	−0.23	−0.22	−0.27	0.10	0.17	−0.04	−0.40	−0.32	0.08	0.20
MPW1K	42.8	0.03	0.24	0.11	−0.02	−0.01	−0.06	0.19	0.38	0.17	−0.26	−0.11	0.11	0.15
MPWB1K	44	−0.08	0.14	0.06	−0.11	−0.22	−0.11	0.04	0.18	0.09	−0.30	−0.09	0.06	0.14
PWB6K	46	−0.06	0.26	0.11	−0.11	0.11	0.00	0.06	0.37	0.10	−0.25	−0.01	0.06	0.15
M08-HX	52.23	−0.38	−0.49	−0.63	−0.65	−0.66	−0.07	−0.19	−0.09	−0.29	−0.31	−0.56	0.28	0.42
M06-2X	54	−0.39	−0.03	−0.19	−0.25	−0.32	−0.04	−0.26	0.11	−0.10	−0.30	−0.37	0.32	0.19
M08-SO	56.79	−0.45	−0.41	−0.55	−0.59	−0.64	−0.03	−0.46	−0.03	−0.21	−0.24	−0.48	0.46	0.35
LC-HCTH/93	0–100	−0.03	0.63	0.54	0.55	0.57	0.83	0.24	1.05	0.75	0.49	0.50	0.14	0.66
LC-M06-L	0–100	−0.03	1.45	1.34	1.39	1.40	1.12	0.26	1.23	1.18	0.84	1.21	0.15	1.24
ωB97	0–100	−0.03	0.32	0.16	0.11	0.01	0.25	0.21	0.48	0.21	−0.01	−0.01	0.12	0.17
ωB97X	15.77−100	−0.05	0.27	0.09	0.08	0.09	0.18	0.14	0.63	0.14	−0.10	−0.09	0.10	0.19
ωB97X-D	22.2−100	−0.06	−0.14	−0.33	−0.45	−0.56	−0.36	0.08	−0.09	−0.33	−0.46	−0.57	0.07	0.37
M11	42.8−100	−0.44	−0.64	−0.77	−0.88	−1.06	−0.44	−0.30	−0.35	−0.42	−0.18	−0.58	0.37	0.59
M06-HF	100	−1.02	0.47	0.32	0.38	0.31	0.84	−0.76	0.69	0.83	0.54	0.67	0.89	0.56
Expt.		4.00	7.08	7.97	8.14	8.37	8.88	9.00	9.22	9.26	9.58	9.63		

[a]For the $1B_1$ $\pi \rightarrow \pi^*$ state, the orbital excited is a nonbonding orbital rather than a π orbital.

TABLE V. Signed errors of vertical electronic excitation energies (eV) for the calculated states of acetaldehyde, and mean unsigned errors (MUEs) for the five Rydberg states.

	X	A″ Val (n-π^*)	2A′ Ryd	3A′ Ryd	4A′ Ryd	6A′ Ryd	7A′ Ryd	MUE(5) Ryd
HCTH/93	0	− 0.06	− 1.47	− 1.68	− 1.64	− 1.91	− 2.07	1.75
M06-L	0	0.30	− 0.98	− 1.26	− 1.23	− 1.53	− 1.71	1.34
SOGGA11	0	− 0.18	− 2.63	− 2.88	− 3.11	− 3.26	− 3.27	3.03
M11-L	0	0.45	− 2.03	− 2.12	− 2.10	− 2.10	− 2.14	2.10
N12-SX	25–0	− 0.04	− 0.64	− 0.81	− 0.81	− 0.96	− 1.14	0.87
MN12-SX	25–0	0.20	− 1.86	− 1.91	− 2.01	− 1.88	− 2.04	1.94
M06	27	− 0.06	− 1.19	− 1.32	− 1.39	− 1.39	− 1.53	1.37
SOGGA11-X	40.15	0.12	0.02	− 0.06	− 0.17	− 0.21	− 0.30	0.15
MPWKCIS1K	41	0.02	0.05	− 0.01	− 0.07	− 0.15	− 0.29	0.12
MPW1K	42.8	0.10	0.28	0.22	0.14	0.05	− 0.08	0.15
MPWB1K	44	− 0.02	− 1.23	− 0.42	− 0.13	− 0.21	− 0.25	0.45
PWB6K	46	0.00	0.19	0.02	− 0.03	− 0.24	− 0.18	0.13
M08-HX	52.23	− 0.28	− 0.47	− 0.44	− 0.59	− 0.40	− 0.46	0.47
M06-2X	54	− 0.32	0.04	0.00	− 0.11	− 0.10	− 0.21	0.09
M08-SO	56.79	− 0.38	− 0.37	− 0.34	− 0.48	− 0.35	− 0.41	0.39
LC-HCTH/93	0–100	0.06	0.77	0.89	0.84	0.88	0.83	0.84
LC-M06-L	0–100	0.07	1.60	1.70	1.51	1.28	1.26	1.47
ωB97	0–100	0.03	0.49	0.50	0.41	0.39	0.25	0.41
ωB97X	15.77–100	0.01	0.39	0.39	0.31	0.27	0.16	0.30
ωB97X-D	22.2–100	0.00	− 0.02	− 0.10	− 0.21	− 0.26	− 0.43	0.21
M11	42.8–100	− 0.36	− 0.52	− 0.50	− 0.63	− 0.47	− 0.67	0.56
M06-HF	100	− 1.04	0.48	0.64	0.48	0.67	0.60	0.58
Expt.		4.28	6.82	7.46	7.75	8.43	8.69	

TABLE VI. Signed errors of vertical electronic excitation energies (eV) for the calculated states of acetone, and mean unsigned errors (MUEs) for the seven Rydberg states.

	X	1A₂ Val (n-π^*)	1B₂ Ryd	2A₂ Ryd	2A₁ Ryd	2B₂ Ryd	3A₁ Ryd	3B₂ Ryd	1B₁ Ryd	MUE(7) Ryd
HCTH/93	0	− 0.14	− 1.48	− 1.68	− 1.86	− 1.71	− 1.68	− 2.08	− 2.02	1.79
M06-L	0	0.25	− 0.93	− 1.28	− 1.48	− 1.37	− 1.46	− 1.72	− 1.67	1.41
SOGGA11	0	− 0.38	− 2.53	− 2.93	− 3.29	− 3.10	− 3.03	− 3.46	− 3.44	3.11
M11-L	0	0.26	− 2.08	− 2.14	− 2.43	− 2.19	− 1.88	− 2.53	− 2.38	2.23
N12-SX	25–0	− 0.06	− 0.58	− 0.81	− 0.94	− 0.84	− 0.68	− 1.14	− 1.03	0.86
MN12-SX	25–0	0.14	− 1.89	− 2.19	− 2.26	− 2.14	− 1.78	− 2.37	− 2.21	2.12
M06	27	− 0.05	− 1.14	− 1.46	− 1.48	− 1.43	− 1.14	− 1.66	− 1.50	1.40
SOGGA11-X	40.15	0.13	0.13	− 0.06	− 0.14	− 0.16	0.07	− 0.37	− 0.20	0.16
MPWKCIS1K	41	0.05	0.16	0.04	− 0.05	− 0.04	0.17	− 0.31	− 0.11	0.12
MPW1K	42.8	0.12	0.41	0.25	0.18	0.17	0.37	− 0.08	0.09	0.22
MPWB1K	44	0.00	0.26	0.08	0.04	0.04	0.32	− 0.13	− 0.16	0.15
PWB6K	46	0.02	0.40	0.29	0.14	0.23	0.39	− 0.23	0.05	0.25
M08-HX	52.23	− 0.23	− 0.33	− 0.46	− 0.43	− 0.53	− 0.11	− 0.61	− 0.28	0.39
M06-2X	54	− 0.30	0.16	− 0.04	− 0.01	− 0.08	0.24	− 0.27	− 0.05	0.12
M08-SO	56.79	− 0.36	− 0.24	− 0.43	− 0.36	− 0.45	− 0.02	− 0.57	− 0.27	0.34
LC-HCTH/93	0–100	0.12	0.96	1.05	1.11	1.01	1.36	0.78	1.10	1.05
LC-M06-L	0–100	0.15	1.69	1.95	1.83	1.87	1.75	1.38	1.08	1.65
ωB97	0–100	0.06	0.72	0.56	0.64	0.52	0.81	0.30	0.51	0.58
ωB97X	15.77–100	0.04	0.57	0.44	0.50	0.39	0.66	0.16	0.37	0.44
ωB97X-D	22.2–100	0.01	0.15	− 0.11	− 0.07	− 0.17	0.08	− 0.37	− 0.22	0.17
M11	42.8–100	− 0.34	− 0.29	− 0.66	− 0.46	− 0.59	− 0.14	− 0.68	− 0.44	0.47
M06-HF	100	− 1.09	0.64	0.49	0.69	0.50	1.00	0.44	0.04	0.54
Expt.		4.43	6.36	7.36	7.41	7.49	7.80	8.09	8.17	

TABLE VII. Signed errors of vertical electronic excitation energies (eV) for the calculated valence states of pyridine.

	X	B_1 Val (n-π^*)	B_2 Val (π-π^*)	A_2 Val (n-π^*)	A_1 Val (π-π^*)	MUE(4) Val
HCTH/93	0	−0.13	0.34	−0.85	−0.22	0.39
M06-L	0	0.17	0.50	−0.51	−0.13	0.33
SOGGA11	0	−0.25	0.35	−1.04	−0.38	0.51
M11-L	0	0.25	0.38	−0.38	−0.61	0.41
N12-SX	25–0	0.23	0.52	−0.23	−0.13	0.28
MN12-SX	25–0	0.39	0.51	−0.01	−0.24	0.29
M06	27	0.15	0.37	−0.37	−0.39	0.32
SOGGA11-X	40.15	0.59	0.67	0.30	0.03	0.40
MPWKCIS1K	41	0.51	0.64	0.20	0.01	0.34
MPW1K	42.8	0.61	0.68	0.35	0.03	0.42
MPWB1K	44	0.50	0.65	0.24	0.04	0.36
PWB6K	46	0.54	0.66	0.32	0.04	0.39
M08-HX	52.23	0.31	0.63	0.09	−0.01	0.26
M06-2X	54	0.28	0.64	0.06	0.17	0.29
M08-SO	56.79	0.23	0.55	0.06	0.17	0.25
LC-HCTH/93	0–100	0.82	0.61	0.53	0.05	0.50
LC-M06-L	0–100	0.78	0.71	0.48	0.26	0.56
ωB97	0–100	0.70	0.60	0.28	0.11	0.42
ωB97X	15.77–100	0.62	0.59	0.20	0.09	0.37
ωB97X-D	22.2–100	0.48	0.57	0.02	0.04	0.27
M11	42.8–100	0.33	0.63	0.07	0.05	0.27
M06-HF	100	0.08	0.76	0.51	0.36	0.43
Expt.		4.59	4.99	5.43	6.38	

TABLE VIII. Signed errors of vertical electronic excitation energies (eV) for the calculated valence states of pyrazine.

	X	B_{3u} Val (n-π^*)	B_{2u} Val (π-π^*)	B_{2g} Val (n-π^*)	B_{1g} Val (n-π^*)	B_{1u} Val (π-π^*)	MUE(5) Val
HCTH/93	0	−0.19	0.41	−0.24	−0.38	−0.13	0.27
M06-L	0	0.06	0.56	0.14	0.08	−0.13	0.19
SOGGA11	0	−0.26	0.46	−0.41	−1.00	−0.14	0.45
M11-L	0	0.16	0.43	0.33	−0.04	−0.52	0.30
N12-SX	25–0	0.13	0.55	0.13	0.45	−0.08	0.27
MN12-SX	25–0	0.33	0.22	0.45	0.01	−0.14	0.23
M06	27	0.04	0.39	0.08	0.36	−0.38	0.25
SOGGA11-X	40.15	0.43	0.67	0.56	1.23	0.08	0.59
MPWKCIS1K	41	0.37	0.65	0.44	1.09	0.06	0.52
MPW1K	42.8	0.46	0.68	0.53	1.07	0.08	0.56
MPWB1K	44	0.37	0.67	0.43	1.16	0.09	0.54
PWB6K	46	0.41	0.67	0.46	1.25	0.08	0.58
M08-HX	52.23	0.21	0.70	0.28	1.02	0.20	0.48
M06-2X	54	0.15	0.68	0.22	1.03	0.21	0.46
M08-SO	56.79	0.10	0.57	0.11	1.03	0.04	0.37
LC-HCTH/93	0–100	0.64	0.55	0.68	1.51	0.08	0.69
LC-M06-L	0–100	0.60	0.68	0.73	1.51	0.28	0.76
ωB97	0–100	0.51	0.56	0.65	1.21	0.14	0.61
ωB97X	15.77–100	0.45	0.57	0.55	1.06	0.12	0.55
ωB97X-D	22.2–100	0.34	0.58	0.41	0.79	0.09	0.44
M11	42.8–100	0.19	0.65	0.25	1.01	0.17	0.45
M06-HF	100	−0.03	0.79	−0.18	0.79	0.38	0.43
Expt.		3.83	4.81	5.46	6.10	6.51	

TABLE IX. Signed errors of vertical electronic excitation energies (eV) for the calculated valence states of pyrimidine.

	X	B$_1$ Val (n-π^*)	A$_2$ Val (n-π^*)	B$_2$ Val (π-π^*)	A$_2$ Val (n-π^*)	B$_1$ Val (n-π^*)	A$_1$ Val (π-π^*)	MUE(6) Val
HCTH/93	0	0.02	−0.51	0.47	−0.29	−0.44	−0.29	0.34
M06-L	0	0.31	−0.21	0.63	0.05	−0.05	−0.16	0.23
SOGGA11	0	−0.12	−0.70	0.45	−0.94	−1.10	−0.30	0.60
M11-L	0	0.45	−0.06	0.52	−0.16	−0.32	−0.73	0.37
N12-SX	25–0	0.47	0.06	0.65	0.18	0.12	−0.19	0.28
MN12-SX	25–0	0.70	0.30	0.70	−0.05	0.42	−0.60	0.46
M06	27	0.37	−0.08	0.52	0.09	0.03	−0.62	0.28
SOGGA11-X	40.15	0.85	0.52	0.83	0.69	0.71	0.01	0.60
MPWKCIS1K	41	0.77	0.43	0.79	0.58	0.59	−0.02	0.53
MPW1K	42.8	0.87	0.56	0.83	0.70	0.74	0.00	0.62
MPWB1K	44	0.77	0.45	0.80	0.59	0.63	0.02	0.54
PWB6K	46	0.82	0.52	0.81	0.65	0.70	0.01	0.58
M08-HX	52.23	0.61	0.30	0.79	0.43	0.43	0.09	0.44
M06-2X	54	0.56	0.26	0.79	0.39	0.43	0.13	0.43
M08-SO	56.79	0.55	0.26	0.71	0.32	0.37	−0.04	0.38
LC-HCTH/93	0–100	1.09	0.74	0.75	0.88	0.85	0.05	0.73
LC-M06-L	0–100	1.03	0.68	0.84	0.86	0.81	0.25	0.74
ωB97	0–100	0.91	0.50	0.73	0.75	0.65	0.10	0.61
ωB97X	15.77–100	0.83	0.43	0.72	0.65	0.57	0.06	0.54
ωB97X-D	22.2–100	0.69	0.27	0.70	0.48	0.41	0.00	0.42
M11	42.8–100	0.62	0.29	0.77	0.40	0.37	0.08	0.43
M06-HF	100	0.56	0.45	0.93	0.51	0.81	0.31	0.60
Expt.		3.85	4.62	5.12	5.52	5.90	6.70	

1. Formaldehyde

Table IV gives signed errors of the vertical transition energies of formaldehyde (point group C$_{2v}$). Two valence states are considered in this molecule, namely, 1A$_2$ $n \to \pi^*$ and 1B$_1$ $\pi \to \pi^*$. The 1A$_2$ state has zero oscillator strength ($f = 0$) by symmetry, and it is described as a HOMO $\to$ LUMO transition by all density functionals except for density functionals that contain a high percentage of Hartree–Fock exchange, in particular M08-SO, ωB97, ωB97X,

TABLE X. Signed errors of vertical electronic excitation energies (eV) for the calculated valence states of pyridazine.

	X	B$_1$ Val (n-π^*)	A$_1$ Val (π-π^*)	A$_2$ Val (n-π^*)	B$_1$ Val (n-π^*)	B$_2$ Val (π-π^*)	MUE(5) Val
HCTH/93	0	−0.37	0.46	−1.68	−0.44	−0.61	0.71
M06-L	0	−0.09	0.61	−1.38	−0.09	−0.29	0.49
SOGGA11	0	−0.54	0.42	−1.91	−1.57	−0.20	0.93
M11-L	0	0.22	−0.41	0.18	−0.24	−0.55	0.32
N12-SX	25–0	−0.03	0.64	−1.10	0.20	−0.29	0.45
MN12-SX	25–0	0.32	0.58	−0.76	−0.21	−0.20	0.41
M06	27	−0.13	0.51	−1.26	0.07	−0.50	0.49
SOGGA11-X	40.15	0.38	0.81	−0.54	0.73	0.04	0.50
MPWKCIS1K	41	0.28	0.77	−0.64	0.63	−0.05	0.48
MPW1K	42.8	0.38	0.81	−0.51	0.78	0.03	0.50
MPWB1K	44	0.28	0.78	−0.61	0.66	0.04	0.47
PWB6K	46	0.33	0.79	−0.54	0.73	0.04	0.49
M08-HX	52.23	0.15	0.79	−0.72	0.48	0.15	0.46
M06-2X	54	0.06	0.78	−0.81	0.46	0.21	0.46
M08-SO	56.79	−0.03	0.70	−0.85	0.45	0.01	0.41
LC-HCTH/93	0–100	0.52	0.73	−0.31	0.97	0.07	0.52
LC-M06-L	0–100	0.50	0.83	−0.36	0.91	0.27	0.57
ωB97	0–100	0.41	0.72	−0.52	0.73	0.13	0.50
ωB97X	15.77–100	0.35	0.71	−0.62	0.63	0.10	0.48
ωB97X-D	22.2–100	0.23	0.69	−0.80	0.45	0.00	0.43
M11	42.8–100	0.08	0.77	−0.77	0.47	0.14	0.45
M06-HF	100	−0.11	0.93	−0.63	0.89	0.41	0.59
Expt.		3.60	5.00	5.30	6.00	6.50	

TABLE XI. Signed errors of vertical electronic excitation energies (eV) for the calculated valence states of s-tetrazine.

	X	B_{3u} Val $(n$-$\pi^*)$	A_u Val $(n$-$\pi^*)$	A_u Val $(n$-$\pi^*)$	B_{3u} Val $(n$-$\pi^*)$	MUE(4) Val
HCTH/93	0	−0.34	−0.48	−0.28	−0.58	0.42
M06-L	0	−0.14	−0.23	−0.09	−0.23	0.17
SOGGA11	0	−0.45	−0.70	−0.69	−0.78	0.66
M11-L	0	0.24	0.14	0.12	0.03	0.13
N12-SX	25–0	0.00	0.15	0.09	0.03	0.07
MN12-SX	25–0	0.40	0.53	0.27	0.35	0.39
M06	27	−0.17	−0.05	−0.09	−0.09	0.10
SOGGA11-X	40.15	0.31	0.67	0.52	0.61	0.53
MPWKCIS1K	41	0.25	0.58	0.43	0.50	0.44
MPW1K	42.8	0.33	0.71	0.53	0.65	0.56
MPWB1K	44	0.25	0.61	0.45	0.53	0.46
PWB6K	46	0.29	0.69	0.49	0.60	0.52
M08-HX	52.23	0.17	0.51	0.38	0.30	0.34
M06-2X	54	0.02	0.41	0.28	0.31	0.25
M08-SO	56.79	−0.04	0.41	0.20	0.26	0.23
LC-HCTH/93	0–100	0.47	0.93	0.72	0.80	0.73
LC-M06-L	0–100	0.43	0.84	0.68	0.71	0.66
ωB97	0–100	0.34	0.67	0.60	0.58	0.55
ωB97X	15.77–100	0.30	0.57	0.50	0.49	0.46
ωB97X-D	22.2–100	0.19	0.39	0.35	0.30	0.31
M11	42.8–100	0.08	0.46	0.32	0.26	0.28
M06-HF	100	−0.04	0.81	0.50	0.77	0.53
Expt.		2.25	3.40	5.00	6.34	

ωB97X–D, M11, and M06-HF, for long-range corrected functionals; LC-HCTH/93 and LC-M06-L. The 1B$_1$ transition is assigned to the lowest B$_1$ calculated transition energy for all density functionals except two of the local density functionals, namely, SOGGA11 and M11-L, although the orbital assigned as a π orbital (HOMO-2 for all density functionals) is a non-bonding orbital. For SOGGA11 and M11-L the lowest B$_1$ transition is from a π orbital to a carbon Rydberg orbital.

MPWKCIS1K, MPW1K, PWB6K, and ωB97X–D have mean unsigned errors below 0.1 eV for the valence states, and MPW1K, MPWB1K, and PWB6K have the best performance for Rydberg states. Although ωB97X–D has a small error for the valence states, it is unsuccessful for the Rydberg states. Table IV shows, for formaldehyde, that 18 of 22 density functionals are successful for the valence states (and one more is moderately successful), and 8 of 22 density functionals are successful for Rydberg states (and again one more is moderately successful).

2. Acetaldehyde

Table V gives signed errors of the vertical transition energies of acetaldehyde (point group C$_s$). The molecular orbitals that contribute to the valence excitation are shown in Fig. 1.

TABLE XII. Overall mean unsigned errors (eV) over 30 valence states, 39 Rydberg states and all 69 transitions for the functionals considered here as compared to the functionals considered by Caricato *et al.*[21]

	X[a]	Valence	Rydberg	Alkenes + carbonyls	Azabenzenes	All states	Reference
EOM-CCSD	WFT	0.47	0.11	0.12	0.53	0.27	Ref. 21
M06-2X	54	0.36	0.26	0.26	0.39	0.30	This work
ωB97X-D	22.2–100	0.32	0.28	0.25	0.39	0.30	This work
MPWKCIS1K	41	0.40	0.27	0.25	0.47	0.32	This work
PWB6K	46	0.43	0.24	0.21	0.52	0.32	This work
CAM-B3LYP	19–65	0.31	0.35	0.32	0.37	0.33	Ref. 21
MPW1K	42.8	0.45	0.23	0.21	0.54	0.33	This work
MPWB1K	44	0.40	0.28	0.25	0.49	0.33	This work
ωB97X	15.77–100	0.40	0.28	0.25	0.49	0.33	This work
BMK	42	0.33	0.39	0.35	0.39	0.36	Ref. 21
M05-2X	52	0.37	0.35	0.34	0.41	0.36	Ref. 21
LC-ωPBE	0–100	0.41	0.32	0.28	0.49	0.36	Ref. 21
B3P86	20	0.19	0.53	0.47	0.21	0.38	Ref. 21

TABLE XII. (*Continued*)

	X^a	Valence	Rydberg	Alkenes + carbonyls	Azabenzenes	All states	Reference
SOGGA11-X	40.15	0.46	0.34	0.32	0.53	0.39	This work
BH&H	50	0.49	0.33	0.30	0.59	0.40	Ref. 21
ωB97	0–100	0.45	0.39	0.34	0.55	0.41	This work
M08-SO	56.79	0.35	0.49	0.48	0.33	0.43	This work
BH&HLYP	50	0.56	0.36	0.33	0.66	0.44	Ref. 21
LC-BLYP	0–100	0.49	0.41	0.37	0.59	0.45	Ref. 21
M08-HX	52.23	0.38	0.51	0.48	0.41	0.46	This work
M11	42.8–100	0.37	0.54	0.51	0.39	0.47	This work
CIS(D)	WFT	0.50	0.49	0.45	0.57	0.49	Ref. 21
M06-HF	100	0.56	0.44	0.48	0.52	0.49	This work
PBE0	25	0.22	0.80	0.71	0.25	0.55	Ref. 21
HSE	25–0	0.21	0.82	0.73	0.24	0.56	Ref. 21
B3P86(VWN5)	20	0.19	0.87	0.77	0.20	0.57	Ref. 21
N12-SX	25–0	0.26	0.85	0.76	0.28	0.59	This work
M05	26	0.24	0.90	0.81	0.25	0.62	Ref. 21
LC-HCTH/93	0–100	0.53	0.70	0.62	0.64	0.63	This work
B3LYP	20	0.20	1.03	0.91	0.20	0.67	Ref. 21
τ-HCTHhyb	15	0.18	1.04	0.92	0.19	0.67	Ref. 21
LC-HCTH/147	0–100	0.53	0.85	0.75	0.64	0.71	This work
LC-HCTH/407	0–100	0.53	0.85	0.75	0.64	0.71	This work
LC-B97-D	0–100	0.53	0.84	0.74	0.64	0.71	This work
M06-L	0	0.28	1.08	0.97	0.28	0.73	This work
TPSSh	10	0.18	1.27	1.12	0.19	0.80	Ref. 21
LC-τ-HCTH	0–100	0.54	1.00	0.88	0.65	0.80	This work
LSDA	0	0.45	1.20	1.08	0.50	0.88	Ref. 21
HCTH/147	0	0.38	1.26	1.12	0.42	0.88	This work
M06	27	0.30	1.33	1.19	0.30	0.88	This work
O3LYP	11.61	0.20	1.47	1.30	0.20	0.92	Ref. 21
B97-D	0	0.39	1.35	1.20	0.43	0.93	This work
VSXC	0	0.24	1.54	1.36	0.25	0.97	Ref. 21
HCTH/93	0	0.38	1.45	1.29	0.42	0.99	This work
HCTH/407	0	0.34	1.51	1.34	0.37	1.00	Ref. 21
τ-HCTH	0	0.32	1.53	1.36	0.34	1.00	Ref. 21
TDHF	WFT	1.19	0.88	0.81	1.39	1.01	Ref. 21
LC-M06-L	0–100	0.57	1.35	1.19	0.67	1.01	This work
TPSS	0	0.26	1.63	1.44	0.27	1.03	Ref. 21
CIS	WFT	1.29	0.91	0.85	1.49	1.07	Ref. 21
BP86	0	0.38	1.62	1.44	0.41	1.08	Ref. 21
BP86(VWN5)	0	0.38	1.62	1.44	0.41	1.08	Ref. 21
PBE	0	0.40	1.70	1.51	0.42	1.13	Ref. 21
BLYP	0	0.40	1.88	1.68	0.41	1.23	Ref. 21
MN12-L	0	0.49	1.80	1.65	0.45	1.23	This work
M11-L	0	0.35	1.93	1.74	0.31	1.24	This work
MN12-SX	25–0	0.38	1.90	1.70	0.36	1.24	This work
N12	0	0.44	1.88	1.68	0.45	1.25	This work
OLYP	0	0.36	1.97	1.76	0.37	1.27	Ref. 21
SOGGA11	0	0.62	2.40	2.15	0.63	1.62	This work

[a]WFT indicates wave function theory; other rows are density functional theory, and X is the percentage of Hartree–Fock exchange. When a range of X is indicated, the first value corresponds to small interelectronic separations, and the second to large interelectronic separations. In Ref. 21, TDHF is labeled RPA.

For the valence transition, 17 functionals are successful (including even one of the local functionals), two is moderately successful, and three are unsuccessful. The statistically best performance for five Rydberg states is given by M06-2X with a MUE of only 0.09 eV., and six other functionals are successful, with 15 unsuccessful. Six functionals are successful for both valence and Rydberg states, and PWB6K and MPWK-CIS1K may especially be singled for excellent performance on both.
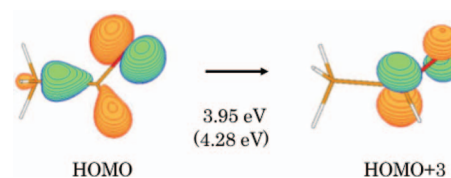

FIG. 1. Molecular orbitals which dominantly contribute to valence transition $n \rightarrow \pi^*$ of acetaldehyde obtained by M06–2X. The calculated transition energy is 3.95 eV as compared to the experimental value of 4.28 eV.

3. Acetone

Table VI gives signed errors of vertical transition energies of acetaldehyde (point group C_{2v}). For all density functionals, the lowest calculated excitation energy in the A_2 irrep is assigned to the $n \rightarrow \pi^*$ valence state. This transition is a HOMO $\rightarrow$ LUMO or HOMO $\rightarrow$ LUMO + 1 transition for the local density functionals, however, the contribution of higher virtual orbitals become significant for this transition as the percentage of Hartree–Fock exchange increases, especially in seven of the density functionals, namely, ωB97, ωB97X, ωB97-D, M11, LC-HCTH/93, LC-M06-L, and M06-HF.

The oscillator strength of the $n \rightarrow \pi^*$ valence state is zero ($f = 0$) by symmetry. The experimental value of the A_2 $n \rightarrow \pi^*$ valence state is reproduced within 0.1 eV by eight functionals, and ten other functionals are successful and two are moderately successful; only two are unsuccessful. The best results for the mean unsigned errors for the seven Rydberg states are attained by (in order of increasing MUE) MPWKCIS1K and M06-2X (tie), then MPWB1K, SOGGA11-X, ωB97X-D, and two other density functionals are also successful (MUE being below 0.3 eV).

We observed large errors (more than 1.0 eV) in the valence states of carbonyl compounds for M06-HF. The transition energies estimated by M06-HF for the A_2 $n \rightarrow \pi^*$ state of formaldehyde, the A'' $n \rightarrow \pi^*$ state of acetaldehyde, and the lowest A_2 $n \rightarrow \pi^*$ state of acetone are 2.98, 3.23, and 3.34 eV as compared to the experimental values of 4.00, 4.28, and 4.43 eV, respectively. These errors are larger than those of TDHF with the 6–311(2+, 2+)G** basis set, for which the calculated transition energies are 4.36, 4.77, and 5.01 eV, respectively. Thus the attempt to use 100% Hartree–Fock exchange in M06-HF, which was successful for closed-shell single-reference ground-state properties, is not reliable for electronic spectroscopy. In this regard we note that Wiberg *et al.*[35] found that TDHF is not satisfactory for formaldehyde, and that is consistent with the poor results for TDM06-HF.

C. Nitrogen heterocycles

Results for nitrogen heterocycles are reported in Tables VII–XI. For these systems, only valence states are considered in the database of Caricato *et al.*

1. Pyridine

Table VII gives the signed errors of the vertical transition energies of pyridine (point group C_{2v}). For pyridine, we consider four valence states, each having a different symmetry. The B_1 $n \rightarrow \pi^*$ state is assigned to the lowest-energy calculated B_1 transition energy for all density functionals except MPWB1K, for which the second lowest energy is assigned because the lowest energy corresponds to a transition from a π orbital to Rydberg orbital ($5s$ of carbon). The B_1 $n \rightarrow \pi^*$ state has an oscillator strength of 0.0029–0.0060. It is a transition from the HOMO or HOMO − 1 to the LUMO or LUMO + 1 for local density functionals, but to higher molecular orbitals (e.g., LUMO + 3) for density functionals that contain Hartree–Fock exchange, and for ωB97, ωB97X,

ωB97XD, M11, and LC-HCTH/93, LC-M06-L, and M06-HF, fairly high virtual orbitals (e.g., LUMO + 5 to LUMO + 20) contribute. This trend was also observed for the $n \rightarrow \pi^*$ valence state of acetone.

The B_2 $\pi \rightarrow \pi^*$ state is assigned to the third lowest-energy calculated B_2 transition energy for SOGGA11 and MPWB1K, to the second lowest one for MN12-SX and M11-L, and to the lowest B_2 energy for the rest of the functionals. The lower calculated energy for SOGGA11 corresponds to a transition from a nonbonding orbital to a Rydberg p orbital of carbon and for MPWB1K to a transition to a Rydberg s orbital of carbon.

The A_2 $n \rightarrow \pi^*$ transition is assigned to the second lowest-energy calculated A_2 transition energy for M11-L (for which the first A_2 transition corresponds to the transition from a π orbital to a Rydberg orbital), to the third lowest to the MN12-SX, to the fifth lowest A_2 state for MPWB1K, and to the lowest energy A_2 state for the remaining density functionals. The oscillator strength of this transition is zero by symmetry.

The A_1 $\pi \rightarrow \pi^*$ transition is assigned to the 8th lowest-energy A_1 state for SOGGA11, to the second lowest-energy A_1 state for N12-SX, M06-L, M06, PWB6K, to the third lowest-energy A_1 state for M11-L and MPWB1K, and to the fifth lowest-energy for MN12-SX. The transition energies lying lower than these correspond to transitions to orbitals with the character of Rydberg s orbitals.

The best performance among all the density functionals for this molecule is given by M08-SO with the MUE being 0.25 eV, and M06-L gives smallest error among the four local density functionals. Overall, seven density functionals are successful, four are moderately successful, and the 11 others are unsuccessful based on the criteria given at the beginning of Sec. III.

2. Pyrazine

Table VIII gives the signed errors of the vertical transition energies of pyrazine (point group D_{2h}), and Fig. 2 shows the molecular orbitals for five valence transitions. The B_{3u} $n \rightarrow \pi^*$ state is assigned to the lowest-energy B_{3u} calculated transition energy for all density functionals except MPWB1K.

The lowest transition energy, described as a transition from the HOMO to the LUMO for all density functionals except LC-HCTH/93, ωB97, ωB97X, M11, and M06-HF, is well separated from the second lowest one.

The B_{2u} $\pi \rightarrow \pi^*$ state is assigned to the second-lowest B_{2u} state for SOGGA11, M11-L, and MPWB1K and to the lowest energy one for the rest of the density functionals. The state lower in energy than the state assigned as valence is a transition from a π orbital to a Rydberg orbital for SOGGA11 and M11-L.

Among the five valence transitions of this molecule, the B_{2u} $\pi \rightarrow \pi^*$ state has the largest oscillator strength with the value being greater than 0.1 for all density functionals except local density functionals SOGGA11 ($f = 0.0339$), M06-L ($f = 0.0822$), HCTH/93 ($f = 0.0740$), and the functionals with
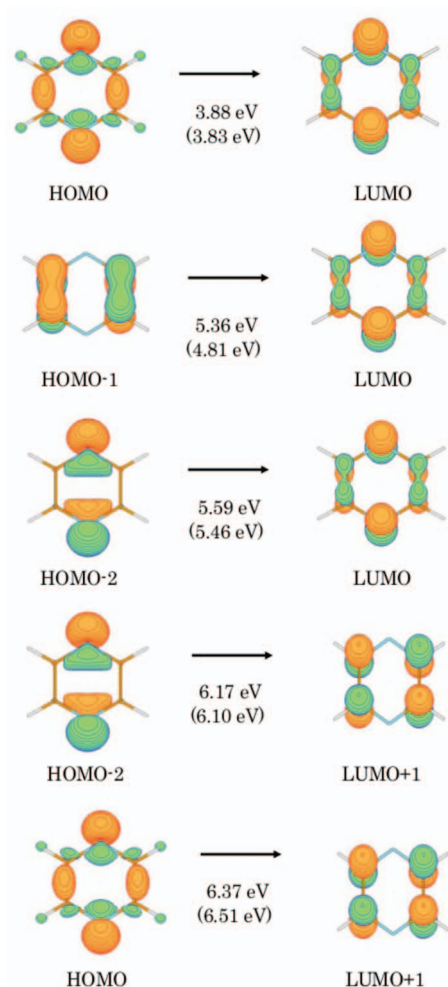
FIG. 2. Molecular orbitals which dominantly contribute to the valence transitions of pyrazine obtained by M06-L. From the bottom up, the orbitals correspond to $n \to \pi^*$, $\pi \to \pi^*$, $n \to \pi^*$, $n \to \pi^*$, $n \to \pi^*$, and $\pi \to \pi^*$, respectively. The experimental value of transition energy is given in parenthesis, under the M06-L values.

low percentage (25% for small range) of Hartree–Fock exchange; N12-SX ($f = 0.0995$), and MN12-SX ($f = 0.0165$).

For the $n \to \pi^*$ B_{2g} state, the lowest transition energy is assigned for all density functionals except for MPWB1K, for which the second lowest energy is assigned. The oscillator strength is zero for by symmetry for B_{2g} and B_{1g} states.

For most density functionals, the lowest B_{1g} state corresponds to excitation from a π orbital to a Rydberg orbital, so the B_{1g} $n \to \pi^*$ transition must be assigned to a higher-energy state, which is the second-lowest state for the MN12-SX, M11-L, M06, MPWCIS1K, PWB6K, M08–HX, M6-2X, M08-SO, and M11 functionals, which as a group exhibit a wide variety of Hartree–Fock exchange percentages. The lowest energy SOGGA11-X transition is $\pi \to \pi^*$.

The B_{1u} $\pi \to \pi^*$ state is the lowest-energy calculated B_{1u} transition except for the HCTH/93, M11-L, MN12-SX and MPWB1K density functionals, for which it is the second lowest, and except for SOGGA11 density functional, for which it is the seventh lowest one. The calculated states that are lower lying than the state assigned as a valence state are mainly Rydberg states. For this state, the oscillator strength is

in the range 0.0437–0.0858 except for M06-L ($f = 0.0002$); these values are small compared with f of the $\pi \to \pi^*$ state for ethylene ($f = 0.1255$–$0.0.4114$ except for SOGGA11 ($f = 0.0001$)).

The best performance is given by M06-L, and the other three local density functionals shows better or comparable performance to the hybrid density functionals. All of the density functionals are unsuccessful for this molecule except for local density functionals; HCTH/93, M06-L, and M11-L, and density functionals with low percentage of Hartree–Fock exchange; N12-SX, MN12-SX, and M06.

3. Pyrimidine

Table IX gives the signed errors of the vertical transition energies of pyrimidine (point group C_{2v}). For the two B_1 $n \to \pi^*$ states, the lowest two transition energies of the B_1 irrep assigned in order of increasing energy for all density functionals except for MN12-SX for which the fourth lowest state is assigned for the second lowest state experimentally observed. We assigned the two lowest A_2 $n \to \pi^*$ states in order of increasing energy for all density functionals.

The B_2 transition is assigned to the lowest calculated transition energy for 15 of the 22 density functionals, to the second lowest for HCTH/93, M06, MPWB1K, and PWB6K, to the third lowest for M11-L and MN12-SX, and to the seventh lowest for SOGGA11.

The A_1 $\pi \to \pi^*$ state is assigned to the second lowest transition energy for HCTH/93, M06-L M11-L, and MN12-SX because the lowest energy transition corresponds to an excitation from a nonbonding orbital to a Rydberg orbital, and to the tenth lowest for SOGGA11, in which all of the lower states are transitions to Rydberg orbital.

Just as for pyrazine, the minimum error for this molecule is given by M06-L, and M08-SO shows the smallest error among hybrid density functionals. For this molecule, only one local density functional, namely, M06-L, and the hybrid density functionals that contains a moderate percentage of Hartree–Fock exchange, namely, M06 and N12-SX, are successful.

4. Pyridazine

Table X gives the signed errors of the vertical transition energies of pyridazine (point group C_{2v}). The lowest and second lowest transition energies of the B_1 irrep are assigned to B_1 $n \to \pi^*$ states.

For the A_1 $\pi \to \pi^*$ state, the sixth transition energy is assigned for SOGGA11, the second transition energy for HCTH/93, M06-L, M11-L, MN12-SX, and M06, and the third transition energy for MPWB1K and PWB6K; the lower-energy calculated states are Rydberg states.

The lowest transition energy of A_2 point group is assigned to the A_2 $n \to \pi^*$.

For the B_2 $\pi \to \pi^*$ state, the 13th lowest energy is assigned for SOGGA11 (in which the lower transition energies correspond to transitions from a nonbonding orbital to a Rydberg orbital), the fifth lowest transition energy is assigned

for M11-L and MN12-SX, the fourth lowest transition energy is assigned for HCTH/93 and M06-L, the third lowest transition energy for M06, the second lowest energy for N12-SX, SOGGA11-X, MPWB1K, PWB6K, M08-HX, M06-2X, M08-SO, and M11, and the lowest transition energy for the rest of the density functionals.

The minimum error is shown by M11-L for this molecule, but all of the hybrid density functionals have similar MUEs, and none of them can be considered successful.

5. s-tetrazine

Table XI gives the signed errors of the vertical transition energies of s-tetrazine, which belongs to the D_{2h} point group. For this molecule, no density functionals yield spurious low-energy states. The oscillator strengths of the A_u states are zero by symmetry, but the oscillator strengths of the B_{3u} $n \to \pi^*$ transitions have a nonzero value. For the A_u states, the higher-energy one has a larger oscillator strength than the lower one.

For this molecule, several local and low-X density functionals; M06-L, M11-L, N12-SX, and M06 perform very well; on the other hand, eight of the hybrid density functionals

and two of long range corrected functionals are unsuccessful, two are only moderately successful, and only three are successful, namely, M08-SO, M06-2X, and M11.

D. Summary

The overall results for the current database, including those obtained by Caricato et al.,[21] are reported in Table XII, and they are plotted in Fig. 3. The functionals in Table XII that have not been considered so far have standard names,[21] but some comments on a few of them might be helpful. BH&H and BH&HLYP are composed of some common parts but put together in different ways. BH&H has 50% Hartree–Fock exchange, 50% Gáspár–Kohn–Sham exchange, and 100% LYP correlation. BH&HLYP has 50% Hartree–Fock exchange, 50% B88 exchange, and 100% LYP correlation. CIS and CIS(D) denote methods from wave function theory (WFT), not DFT. In particular CIS denotes configuration interaction with single excitations,[63] and CIS(D) indicates CIS plus perturbative double excitations.[64] Whereas methods were listed in previous tables in order of increasing X, in Table XII they are listed in order of increasing overall MUE.
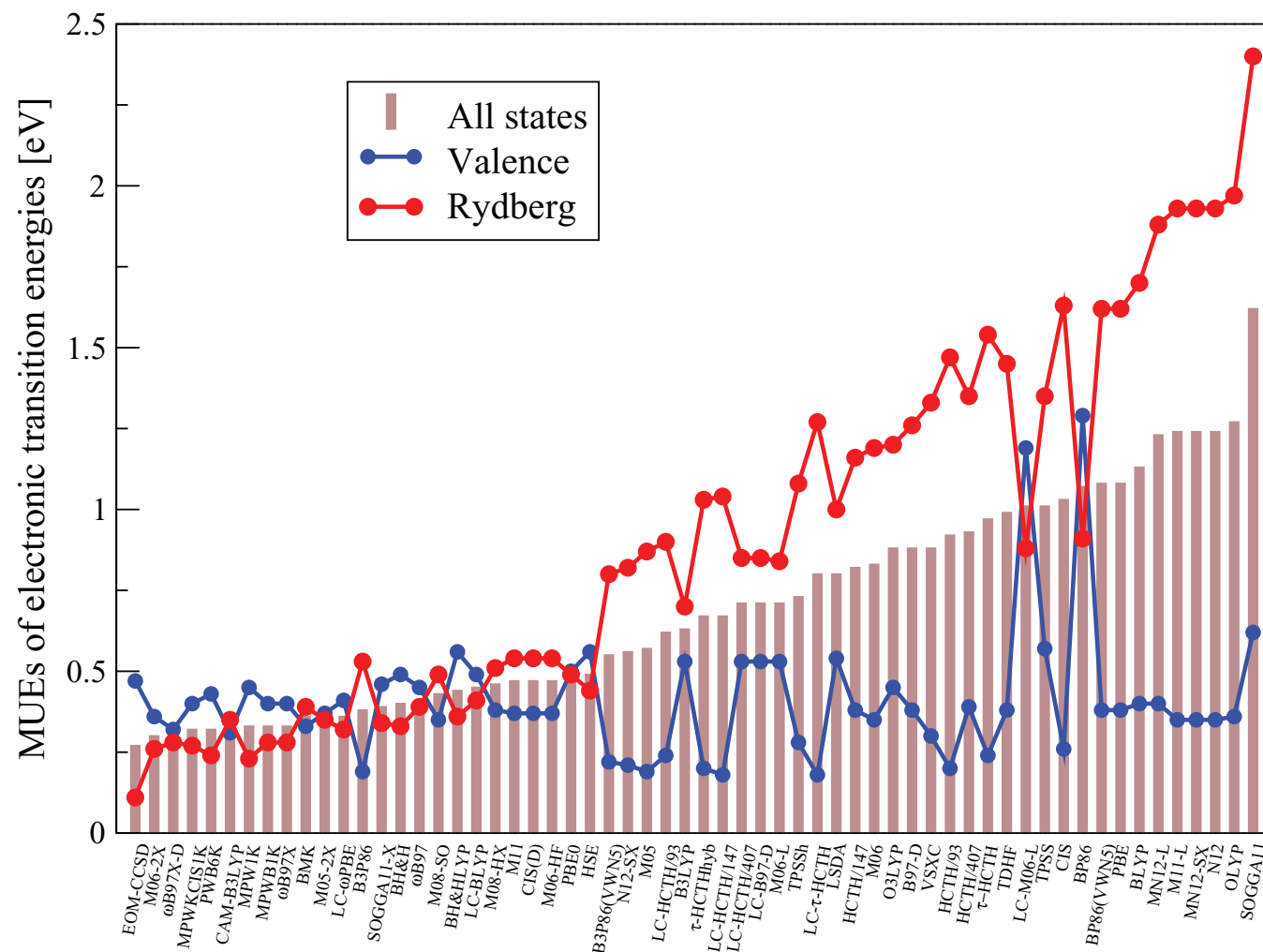

FIG. 3. Mean unsigned errors (in eV) of vertical transition energies for 30 valence states and 39 Rydberg states (as compared to experimental data in the database of Caricato et al.[21]) for 56 density functionals and four wave function methods.

For the 30 valence states, many of the functionals provide successful results (i.e., MUE $\leq$ 0.30 eV): τ-HCTH, TPSSh, B3P86, B3P86 with the VWN No. 5 functional for the local-spin-density part of the correlation term (this is called B3VP86 in Ref. 21), B3LYP, O3LYP, HSE, PBE0, VSXC, M05, N12-SX, TPSS, M06-L, and M06; in general, functionals that have a high percentage of HF exchange are worse for these transitions, and among the leading functionals for valence transitions, the one with the highest percentage of HF exchange is M06 (which has $X = 27$). Among the total of 56 density functional methods considered, 14 provide performance for valence states within 0.30 eV, showing that TDDFT can be rather successful for valence excitations, while a total of 23 are within 0.36 eV, and 47 are within 0.50 eV.

The situation changes for the 39 Rydberg transitions, for which seven density functional methods are successful (MUE $\leq$ 0.30 eV), namely: M06-2X, ωB97X-D, MPWK-CIS1K, PWB6K, MPW1K, MPWB1K, and ωB97X. Considering MUEs within 0.50 eV we notice that all DFT methods satisfying this criterion are either hybrid functionals with a percentage of HF exchange larger than 40% or range-separated hybrid functionals. WFT in the form of EOM-CCSD is best performer for Rydberg transitions (MUE = 0.11 eV), although its MUE of 0.47 eV for valence transitions is disappointing. Local functionals are particularly bad for Rydberg transitions, and as we noted above, they also suffer from the problem of spuriously lowered states.

It is notable that the application of long-range correction to Handy's functionals, HCTH/93, HCTH/147, HCTH/407, and τ-HCTH (see the supplementary material[61]), improves the description of Rydberg states ($\sim$0.5 eV), however, the errors become somewhat larger for valence states. On the other hand, the LC correction does not improve M06-L, in which the description of both valence and Rydberg transitions becomes worse, implying that the parameters in Eq. (1) are not general and that the LC correction provides less improvement for functionals whose performance is already better than average.

The statistics illustrate that functionals with an intermediate percentage of Hartree–Fock exchange (about 40%–55%) perform best when one considers both valence and Rydberg states. Naturally, one wants to understand this on the basis of general principles, and it is tempting to oversimplify the arguments to do so; but the reader should keep in mind that there are many factors involved and they are not completely understood. For example, it is very popular to explain the relative accuracy of various density functionals for spin-change excitations almost entirely in terms of Hartree–Fock exchange, but more detailed analysis shows that the true situation is more complicated.[65] With this as a caveat, we present the following necessarily oversimplified explanation of some of the key trends. First of all we know that high amounts of Hartree–Fock exchange cause static correlation error[66] and for ground states one would not recommend functionals with a percentage X of Hartree–Fock exchange more than about 20–30 (depending on the rest of the functional) for systems with high multireference character. Static correlation error is usually caused by near degeneracies. For ground states, the usual situation (although exceptions are well known) is that the ground state is separated from the rest of the spectrum by a large gap, so near-degeneracy correlation is minimal. For excited states, the spectrum is much denser, and near degeneracy is the norm rather than the exception. Thus most excited states have near-degeneracy correlation. All other factors being equal, this would tend to demand the lowest possible X. But if we lower X all the way down to zero we increase other errors due to small HOMO-LUMO gaps, overbinding, and overestimation of delocalization due to self-interaction. The best compromise for valence states seems to be X of about 25 ± 5.[5,8] But this is clearly not high enough for Rydberg states, which seem to demand that X (when treated as a global constant) be $\sim$50 or higher in order to reduce the effect of self-interaction on the character of the effective potential at large distances from the nuclei. If one makes X that high though, the valence states start becoming inaccurate due to static correlation error. If one wants a functional with reasonable performance for both valence and Rydberg states, then the best compromise between X equal to 25 ± 5 and X greater than 50 seems to be X in the range 40–45, and that explains (in part) the good performance of MPW1K and PWB1K. One should not oversimplify though because setting X in that range is safer with some functionals that others. For example, it was known a long time ago that the mPW functional has better overall performance with high X than does the BLYP functional,[42] and that meta functionals, if properly designed to work well with given value of X, work better over a broad range of X than do GGAs.[13] In the context of the above, some readers might be surprised that the so-called LC functionals do not do better for Rydberg states, especially those with X equal to 100 at large interelectronic separations. One should keep in mind though that these functionals still have $X < 50$ at small interelectronic separation, and their range separation parameters were not optimized for Rydberg states. At this point, we repeat the warning that explanations such as the above are necessarily oversimplified, since the real situation involves competing factors that contribute to accuracy or inaccuracy in various ways.

IV. CONCLUSIONS

A very important lesson learned in the present study, as well as a previous one,[8] is that we draw different conclusions from a balanced data set containing both valence and Rydberg states than one draws from earlier work employing primarily valence excitations. Since most excited states of most molecules are Rydberg states, Table XII should provide very useful guidance for applications that are not restricted to valence states. The overall results, looking simultaneously at valence and Rydberg states, are strongly influenced by poor DFT performances for the Rydberg states; nevertheless, two of the 56 functionals in Table XII and EOM-CCSD have a MUE less than or equal to 0.30 eV. Among the total of 23 methods (21 DFT and two WFT) with a MUE below 0.50 eV there is no local functional, and expanding the limit to 0.90 eV, M06-L and LSDA are the only local functionals to be in the list. Eleven density functionals, four range-separated with $X \geq 65$ at large interelectronic separation and seven global hybrids with X in the range 41–54, are successful or moderately successful (MUE $\leq$ 0.36): the global hybrids

are M06-2X, MPWKCIS1K, PWB6K, MPW1K, MPWB1K, BMK, M05-2X, and the range-separated ones are ωB97X-D, LC-ωPBE, CAM-B3LYP, and ωB97X.

In choosing among the eight best performing density functionals in the overall assessment of Table XII (the ones with MUEs for all states in the range 0.30–0.33 eV), one might want to take account of some additional considerations over and above the differences in MUEs. For example, one of the eight functionals, namely MPW1K, is particularly simple (and therefore easier to port to a great variety of electronic structure packages), being a global hybrid GGA with no range separation and no kinetic energy density; however, slightly lower in the list (MUE = 0.39 eV) we find SOGGA11-X, which has better overall performance[39] on a broad chemistry database. Three of the eight most successful functionals, namely, ωB97X-D, ωB97X, and CAM-B3LYP are range separated; this makes them more complicated, but it also means they are expected to have better performance for long-range charge transfer states, which are not considered here, and this is an important consideration in interpreting an entire spectrum. The other four functionals, namely, M06-2X, MPWKCIS1K, PWB6K, and MPWB1K are global hybrid meta-GGAs. Such functionals in general have better across the board performance than the simpler global hybrid GGAs, but they sometimes require finer grids or extra patience in achieving SCF convergence. However, M06-2X has proved to be useful and accurate for many ground-electronic-state problems, and so it could be a good choice for treating ground and excited states on a consistent basis, as—for the same reason—could M05-2X (MUE = 0. 36 eV).

The quest for a universally applicable functional continues, but at present readers would be well advised not to use the functionals in the lower reaches of Table XII for applications in electronic spectroscopy or photochemistry.

ACKNOWLEDGMENTS

[1] E. Gross and W. Kohn, Adv. Quantum Chem. **21**, 255 (1990); M. A. L. Marques and E. K. U. Gross, Annu. Rev. Phys. Chem. **55**, 427 (2004).
[2] M. E. Casida, *Recent Advances in Density Functional Methods. Part I*, edited by D. P. Chong (World Scientific, Singapore, 1995), p. 155.
[3] R. Bauernschmitt and R. Ahlrichs, Chem. Phys. Lett. **256**, 454 (1996).
[4] R. E. Stratmann, G. E. Scuseria, and M. J. Frisch, J. Chem. Phys. **109**, 8218 (1998).
[5] D. Jacquemin, V. Wathelet, E. A. Perpète, and C. Adamo, J. Chem. Theory Comput. **5**, 2420 (2009).
[6] M. R. Silva-Junior, M. Schreiber, S. P. A. Sauer, and W. Thiel, J. Chem. Phys. **129**, 104103 (2008).
[7] A. V. Marenich, C. J. Cramer, D. G. Truhlar, C. A. Guido, B. Mennucci, G. Scalmani, and M. J. Frisch, Chem. Sci. **2**, 2143 (2011).
[8] D. Jacquemin, E. A. Perpète, I. Ciofini, C. Adamo, R. Valero, Y. Zhao, and D. G. Truhlar, J. Chem. Theory Comput. **6**, 2071 (2010).
[9] R. Peverati and D. G. Truhlar, J. Phys. Chem. Lett. **2**, 2810 (2011).
[10] D. Jacquemin, Y. Zhao, R. Valero, C. Adamo, I. Ciofini, and D. G. Truhlar, J. Chem. Theory Comput. **8**, 1255 (2012).
[11] Y. Zhao and D. G. Truhlar, J. Chem. Phys. **125**, 194101 (2006).
[12] Y. Zhao and D. G. Truhlar, J. Phys. Chem. A **110**, 13126 (2006).
[13] Y. Zhao and D. G. Truhlar, Theor. Chem. Acc. **120**, 215 (2008).
[14] Y. Zhao and D. G. Truhlar, J. Chem. Theory Comput. **4**, 1849 (2008).
[15] R. Peverati and D. G. Truhlar, Phys. Chem. Chem. Phys. **14**, 11363 (2012).
[16] R. Peverati and D. G. Truhlar, J. Phys. Chem. Lett. **3**, 117 (2012).
[17] R. Peverati and D. G. Truhlar, J. Chem. Theory Comput. **8**, 2310 (2012).
[18] R. Peverati and D. G. Truhlar, Phys. Chem. Chem. Phys. **14**, 13171 (2012).
[19] R. Peverati and D. G. Truhlar, Phys. Chem. Chem. Phys. **14**, 16187 (2012).
[20] J. Heyd, G. E. Scuseria, and M. Ernzerhof, J. Chem. Phys. **118**, 8207 (2003).
[21] M. Caricato, G. W. Trucks, M. J. Frisch, and K. B. Wiberg, J. Chem. Theory Comput. **6**, 370 (2010).
[22] L. Goerigk, J. Moellmann, and S. Grimme, Phys. Chem. Chem. Phys. **11**, 4611 (2009).
[23] S. S. Leang, F. E. Zahariev, and M. S. Gordon, J. Chem. Phys. **136**, 104101 (2012).
[24] C. A. Ullrich and K. Burke, J. Chem. Phys. **121**, 28 (2004).
[25] F. Wang and T. Ziegler, J. Chem. Phys. **121**, 12191 (2004).
[26] M. E. Casida, J. Chem. Phys. **122**, 054111 (2005).
[27] P. Elliott, S. Goldson, C. Canahui, and N. T. Maitra, Chem. Phys. **391**, 110 (2011).
[28] A. Ipatov, A. Heßelmann, and A. Görling, Int. J. Quantum Chem. **110**, 2202 (2010).
[29] Y. Shao, M. Head-Gordon, and A. I. Krylov, J. Chem. Phys. **118**, 4807 (2003).
[30] M. Huix-Rotllant, B. Natarajan, A. Ipatov, C. Muhavini Wawire, T. Deutsch, and M. E. Casida, Phys. Chem. Chem. Phys. **12**, 12811 (2010).
[31] K. Yang, R. Peverati, D. G. Truhlar, and R. Valero, J. Chem. Phys. **135**, 044118 (2011).
[32] R. Valero, F. Illas, and D. G. Truhlar, J. Chem. Theory Comput. **7**, 3523 (2011).
[33] A. T. B. Gilbert, N. A. Besley, and P. M. W. Gill, J. Phys. Chem. A **112**, 13164 (2008).
[34] T. Ziegler, M. Krykunov, and J. Cullen, J. Chem. Phys. **136**, 124107 (2012).
[35] K. B. Wiberg, A. E. de Oliveira, and G. Trucks, J. Phys. Chem. A **106**, 4192 (2002).
[36] Y. Zhao, R. Peverati, K. Yang, and D. G. Truhlar, MN-GFM, Version 6.3: Minnesota Gaussian Functional Module, University of Minnesota, Minneapolis (2012).
[37] M. J. Frisch, G. W. Trucks, H. B. Schlegel *et al.*, GAUSSIAN 09, Revision A.1, Gaussian, Inc., 2009.
[38] R. Peverati, Y. Zhao, and D. G. Truhlar, J. Phys. Chem. Lett. **2**, 1991 (2011).
[39] R. Peverati and D. G. Truhlar, J. Chem. Phys. **135**, 191102 (2011).
[40] J.-D. Chai and M. Head-Gordon, J. Chem. Phys. **128**, 084106 (2008).
[41] J.-D. Chai and M. Head-Gordon, Phys. Chem. Chem. Phys. **10**, 6615 (2008).
[42] B. J. Lynch, P. L. Fast, M. Harris, and D. G. Truhlar, J. Phys. Chem. A **104**, 4811 (2000).
[43] Y. Zhao and D. G. Truhlar, J. Phys. Chem. A **108**, 6908 (2004).
[44] Y. Zhao, N. González-García, and D. G. Truhlar, J. Phys. Chem. A **109**, 2012 (2005).
[45] Y. Zhao and D. G. Truhlar, J. Phys. Chem. A **109**, 5656 (2005).
[46] F. A. Hamprecht, A. J. Cohen, D. J. Tozer, and N. C. Handy, J. Chem. Phys. **109**, 6264 (1998).
[47] S. Grimme, J. Comput. Chem. **27**, 1787 (2006).
[48] A. D. Boese and N. C. Handy, J. Chem. Phys. **114**, 5497 (2001).
[49] A. D. Boese and N. C. Handy, J. Chem. Phys. **116**, 9559 (2002).
[50] H. Iikura, T. Tsuneda, T. Yanai, and K. Hirao, J. Chem. Phys. **115**, 3540 (2001).
[51] J.-W. Song, T. Hirosawa, T. Tsuneda, and K. Hirao, J. Chem. Phys. **126**, 154105 (2007).
[52] R. Kobayashi and R. D. Amos, Chem. Phys. Lett. **420**, 106 (2006).
[53] Y. Tawada, T. Tsuneda, S. Yanagisawa, T. Yanai, and K. Hirao, J. Chem. Phys. **120**, 8425 (2004).
[54] M. E. Casida, C. Jamorski, K. C. Casida, and D. R. Salahub, J. Chem. Phys. **108**, 4439 (1998).
[55] D. J. Tozer and N. C. Handy, J. Chem. Phys. **109**, 10180 (1998).
[56] A. Gaiduk, D. Firaha, and V. N. Staroverov, Phys. Rev. Lett. **108**, 253005 (2012).
[57] A. Lange and J. M. Herbert, J. Chem. Theory Comput. **3**, 1680 (2007).
[58] A. W. Lange and J. M. Herbert, J. Am. Chem. Soc. **131**, 3913 (2009).
[59] A. J. A. Aquino, D. Nachtigallova, P. Hobza, D. G. Truhlar, C. Hättig, and H. Lischka, J. Comput. Chem. **32**, 1217 (2010).
[60] T. H. Dunning, Jr., W. J. Hunt, and W. A. Goddard III, Chem. Phys. Lett. **4**, 147 (1969); R. J. Buenker, S. Peyerimhoff, W. E. Kammer, and H. Hsu, *ibid.* **8**, 129 (1971); C. F. Bender, T. H. Dunning, Jr., H. F. Schaefer III, W. A. Goddard III, and W. J. Hunt, *ibid.* **15**, 171 (1972); R. J. Buenker and S. Peyerimhoff, *ibid.* **69**, 7 (1980); E. R. Davidson, J. Phys. Chem. **100**, 6161 (1996); D. J. Tozer, R. D. Amos, N. C. Handy, B. O. Roos, and L.

Serrano-Andres, Mol. Phys. **97**, 859 (1999); M. Dallos and H. Lischka, Theor. Chem. Acc. **112**, 16 (2004); C. Angeli, S. Borini, L. Ferrighi, and R. Cimiraglia, J. Chem. Phys. **122**, 114304 (2005); C. Angeli, J. Comput. Chem. **30**, 1319 (2009); R. Send, M. Kühn, and F. Furche, J. Chem. Theory Comput. **7**, 2376 (2011).

[61] See supplementary material at http://dx.doi.org/10.1063/1.4769078 for versions of Tables I–XI that include all 30 newly tested density functionals and a version of Table XII that includes the maximum error.

[62] D. C. Comeau and R. J. Bartlett, Chem. Phys. Lett. **207**, 414 (1993).

[63] J. B. Foresman, M. Head-Gordon, J. A. Pople, and M. J. Frisch, J. Phys. Chem. **96**, 135 (1992).

[64] M. Head-Gordon, R. J. Rico, M. Oumi, and T. J. Lee, Chem. Phys. Lett. **219**, 21 (1994).

[65] S. Luo and D. G. Truhlar, J. Chem. Theory Comput. **8**, 4112 (2012).

[66] M. A. Buijse and E. J. Baerends, J. Chem. Phys. **93**, 4129 (1990).